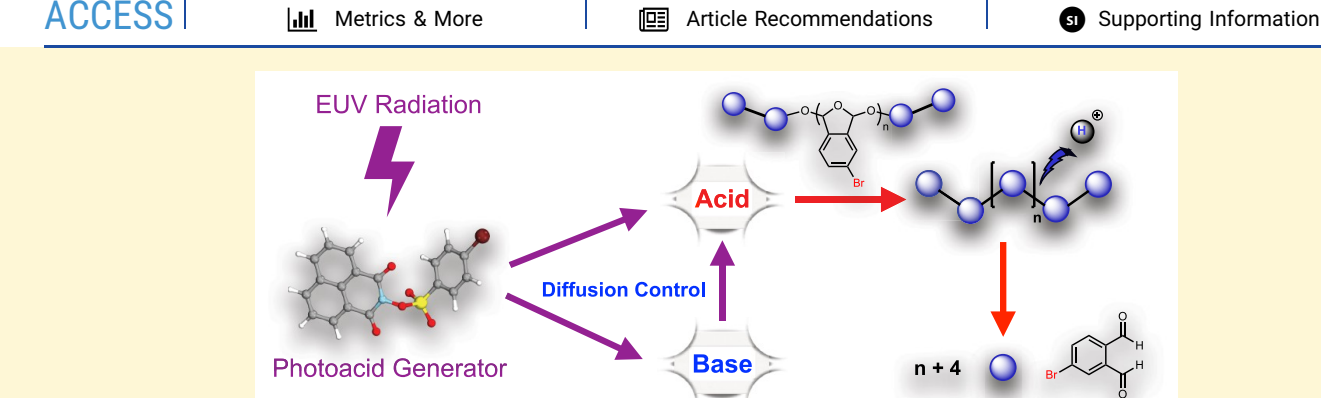


pubs.acs.org/cm Article

# High-Performance Chain Scissionable Resists for Extreme Ultraviolet Lithography: Discovery of the Photoacid Generator Structure and Mechanism

Jingyuan Deng,\* Sean Bailey, Shaoyi Jiang, and Christopher K. Ober\*





ABSTRACT: Extreme ultraviolet (EUV) lithography currently dominates the frontier of semiconductor fabrication. Photoresists must satisfy increasingly strict pattern fidelity requirements to realize the significant enhancements in resolution offered by EUV technology. Traditional chemically amplified resists (CARs) have hit a barrier in the form of the resolution, line edge roughness, and sensitivity trade-off. This has been compounded by a lack of understanding of the chemical mechanism associated with the EUV process. Here, we synthesize a series of novel EUV photoresists based on a self-immolative, acid-labile poly(acetal) system. These systems are shown to be commercially viable under current EUV requirements. Careful study of the resists' degradation pathways has enabled the identification of a remarkable photoacid generator (PAG) that functions as both an acid generator and base quencher, enabling further improvements over previous resists. density functional theory calculations reveal, for the first time, the connection between the PAG activation barrier and resist sensitivity and suggests why attempts to use electron-beam lithography to predict EUV performance have failed.

#### INTRODUCTION

To meet future miniaturization requirements of the semiconductor industry, the development of photoresists that achieve the goals of the International Roadmap for Devices and Systems (IRDS) targets of sub-10 nm resolution, sensitivity below 20 mJ/cm<sup>2</sup>, and line edge roughness (LER) less than 20% will be critical.<sup>1,2</sup> Achieving these goals is dependent upon the increased understanding of chemical mechanisms associated with exposure to extreme ultraviolet (EUV) radiation, the industry's next-generation 13.5 nm patterning wavelength. Almost all commercially relevant EUV photoresists are positive or negative tone chemically amplified resists (CARs).<sup>3-7</sup> CARs were first invented by IBM in the 1980s<sup>8</sup> and incorporate polymers containing acid-sensitive protecting groups, photoacid generators (PAGs), and base quenchers. Upon exposure to 13.5 nm light, the PAGs dissociate into strong acids that can deprotect the polymer and alter its solubility such that the exposed region can be removed in a basic developer, which is commonly an aqueous solution of tetramethylammonium hydroxide. As this process is catalytic, each photogenerated acid is capable of deprotecting multiple groups on the polymer. The function of the base quencher is to limit the diffusion of the acids into unwanted regions and to improve LER.

Unfortunately, CARs relying on deprotection to generate a solubility difference have been found to be limited by the need for acid diffusion to induce deprotection, resulting in a trade-off between resolution, LER, and sensitivity (RLS).<sup>9,10</sup> The RLS trade-off is fundamentally linked to the sharpness of the solubility gradient in the exposed region of the resist. <sup>11,12</sup> As an enhancement of the gradient is hampered by the stochastics of

Received: May 12, 2022 Revised: June 20, 2022 Published: June 30, 2022





Scheme 1. Scheme Showing Chemical Structures of PPA Derivatives

#### **Previous work**

#### This work

the deprotection process, CARs have struggled to overcome this barrier. Many novel resist architectures <sup>13–15</sup> and photo-lithographic techniques <sup>16–18</sup> have emerged because of this issue, and two established methods of overcoming the RLS trade-off were developed. The first method increases the effective reaction radius for the deprotection process while simultaneously increasing the diffusional barrier of the acid.<sup>19</sup> While this strategy is difficult to implement when deprotection is used as the solubility switch, a different class of photoresists, namely chain-scissionable polymers<sup>20-24</sup> that depolymerize upon removal of their end-cap or cleavage of their backbone linkages, is capable of realizing the full potential of this method. This prospect results from the low activation energy required for the removal of many monomeric units relative to a deprotection-based system. Additionally, the anisotropic diffusion of PAGs in the exposed area of chain-scissionable resists is further expected to improve the solubility gradient.<sup>23</sup>

One of the most well-known depolymerizable photoresists is poly(phthalaldehyde) (PPA). PR Recently, there have been several attempts to utilize PPA as an EUV resist, 26,27 but none have been successful. This result is due to the instability of PPA contributing to dark loss and contamination of the EUV optics due to the outgassing of the highly volatile monomers of PPA. As few other chain-scissionable polymers exist that display similarly high rates of depolymerization in the solid state, it is not surprising that the number of EUV resists based on depolymerization has been few, with many promising candidates having issues such as optics contamination, as in the case of poly(sulfones), or low sensitivity, as in the case of poly(carbonates).

The second established method of overcoming the RLS trade-off is to increase the PAG concentration, thereby increasing the efficiency of the exposure process and reducing

shot noise effects. 9,10,31,32 However, this approach is restricted as EUV resists almost exclusively implement ionic PAGs that may segregate from the polymer, especially at concentrations above 20 wt %.33 While nonionic PAGs have been thoroughly investigated<sup>34–36</sup> and shown to outperform ionic PAGs in several areas including dark loss, 35,37 acid generation under e-beam conditions, 34,37 outgassing, 38 and PAG phase separation,<sup>39</sup> a few nonionic PAG are capable of achieving sub-20 mJ/cm<sup>2</sup> sensitivity under EUV exposure. This sensitivity challenge has been exacerbated by the limited mechanistic knowledge of the EUV process, especially with respect to the behavior of nonionic PAGs. While the acid generation efficiency of nonionic PAGs has been demonstrated to strongly correlate with the PAGs' electron affinity under e-beam conditions, 34,40-43 such a trend has been consistently violated 44,45 when the exposure source has been changed to EUV. Many authors have recently speculated on the potential origin of this anomalous behavior, 44,46 but no substantial evidence has been provided. Because the initial step in the decomposition of nonionic PAGs is the formation of a radical anion, it has been exceptionally difficult to explore these multiconfigurational systems using traditional density functional theory (DFT).

Herein, we describe the design and synthesis of eleven photoresists consisting of a PPA derivative and a nonionic PAG. Several of these display high stability, low outgassing, and unprecedented sensitivity under EUV exposure. These resist systems will enable us to take advantage of both methods of bypassing the RLS trade-off. The unusual contrast curve behavior of two PAGs motivated us to elucidate their EUV decomposition products, and in the process, we discovered that the PAGs could simultaneously generate both acid and base, demonstrating a novel mechanism that will improve the

#### Scheme 2. Scheme Showing Chemical Structures of PAG 1 to 9

Scheme 3. Scheme Showing Synthetic Pathways for the Brominated oPA Monomer and Photoacid Generators (PAGs)

Scheme 4. Scheme Showing Anionic Polymerization of Brominated oPA to Form P1

LER of future photoresists by eliminating the stochastics of quencher distribution. Lastly, we illuminate the EUV mechanism of the nonionic PAGs using Fermi-Smearing techniques (FT-DFT) to deal with the multiconfigurational system and explain the sensitivity trend.

#### ■ RESULTS AND DISCUSSION

Synthesis of Monomers, Polymers, and PAGs. Both the synthesis and application of the original ortho-phthaldehyde (oPA) polymer have been extensively studied as it is commercially available from major chemical suppliers. 28,47,48 In contrast, oPA derivatives have rarely been explored due to synthetic challenges (Scheme 1).<sup>49</sup> Commercially acceptable photoresists have high purity requirements, which motivated us to explore simple, high-yielding reactions and thorough methods of purification. We chose to prepare a brominated derivative from the corresponding diol via Swern oxidation as all other means of oxidation failed to generate the desired product in acceptable yield due to the formation of lactone side products. After reaction condition optimization, the overall yield was improved to 72%, which was acceptable for large-scale synthesis. Additionally, we discovered that repeated sublimation under vacuum at 120 °C (as opposed to oPA, which is highly volatile and can be sublimed at 40 °C under vacuum) offered superior purity to column chromatography and enabled scaling up to 50 g (Scheme 3).

We designed the PAGs based first on known deep ultraviolet (DUV) active moieties including aryl, naphthalimide, and iminosulfonates<sup>35</sup> with the hope that some would show activity under EUV and could be subsequently optimized via rational structural variations. The PAGs were synthesized through a simple condensation reaction in quantitative yields (Scheme 3). To ensure maximum purity and ease of scale-up, recrystallizing solvent systems were established for all PAGs. The brominated oPA could be polymerized through both anionic and cationic initiation to afford linear and cyclic polymers, respectively. Cyclic brominated PPA (Br-cPPA) was synthesized using BF3·EtO2 as previously reported for the synthesis of cyclic PPAs. 50 However, the reaction could only generate the cyclic polymer in 25-30% yield. This yield was unacceptable for large-scale synthesis and likely due to the electron-withdrawing nature of the bromine atom. In sharp contrast, linear brominated PPA (Br-lPPA) could be obtained using an alcoholic initiator combined with a DBU base in 70-80% yield (Scheme 4). We found no significant difference in lithographic performance using either the cyclic or linear polymer (Supporting Information). The advantage of the linear polymer is that its reactivity could be finely tuned by changing the end-cap of the polymer. <sup>28</sup> In this work, we chose to end-cap the linear brominated PPA using phenyl chloroformate as opposed to the popular acetyl anhydride to create a carbonate bond linkage rather than an ester bond linkage at the end of the polymer, as EUV radiation is known

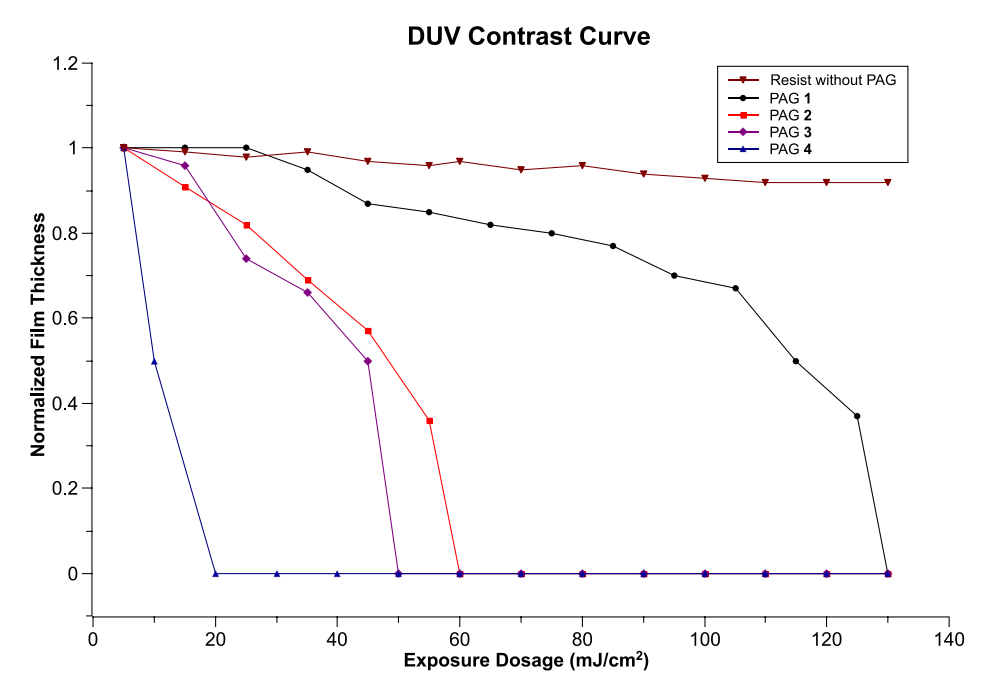


Figure 1. DUV contrast curves for PAG 1-4.

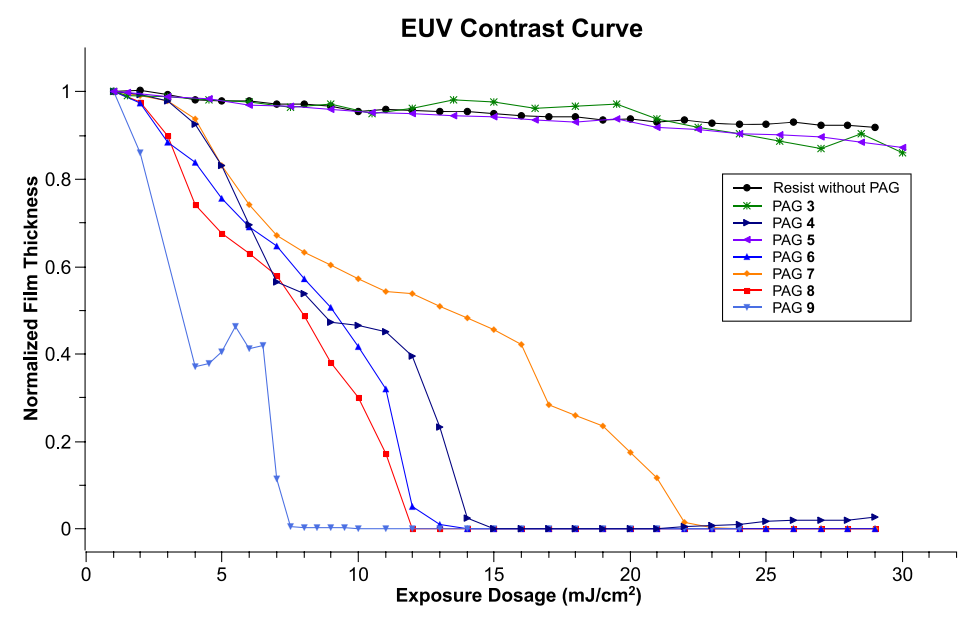


Figure 2. EUV contrast curves for PAG 3-9.

to cleave carbonate linkages. In the most ideal case, the phenyl chloroformate end-capped Br-lPPA could function as a single component photoresist that would not require the use of PAGs as the depolymerization process is a thermodynamic sink after end-cap removal. Unfortunately, we observed minimal film thickness decline in its EUV contrast curve up to  $30~\text{mJ/cm}^2$ , indicating that the carbonate linkage at the end of the polymer could not be cleaved under commercially relevant dosages, possibly due to the weak sensitivity of the carbonate bond or the scarce number of EUV photons to precisely reach the end of the polymer.

Significantly improved thermostability was observed on Br-*l*PPA in comparison to *c*PPA. From thermogravimetric analysis (TGA, Supporting Information), *c*PPA showed 5% weight loss at 128 °C, whereas Br-*l*PPA showed 5% weight loss at 178 °C.

The superior thermostability of Br-IPPA indicated that higher postexposure bake temperatures could be applied and that outgassing would no longer be a significant issue. This was confirmed under EUV exposure with in situ MS (Supporting Information) and demonstrated that the only detectable outgassing product was CO<sub>2</sub>, which does not significantly contribute to contamination of exposure optics. <sup>51</sup>

**DUV Exposure.** Although photoresists exposed to DUV light at 248 nm show completely different behavior when exposed to EUV light due to the difference in acid generation mechanism, <sup>52</sup> we used DUV exposure as a method of screening resist systems for pattern generation and processing condition optimization. PAGs **1–4** (Scheme 2) were combined with Br-*I*PPA in a 20 wt % ratio (mol % conversions are listed in the Supporting Information, Table S1) and

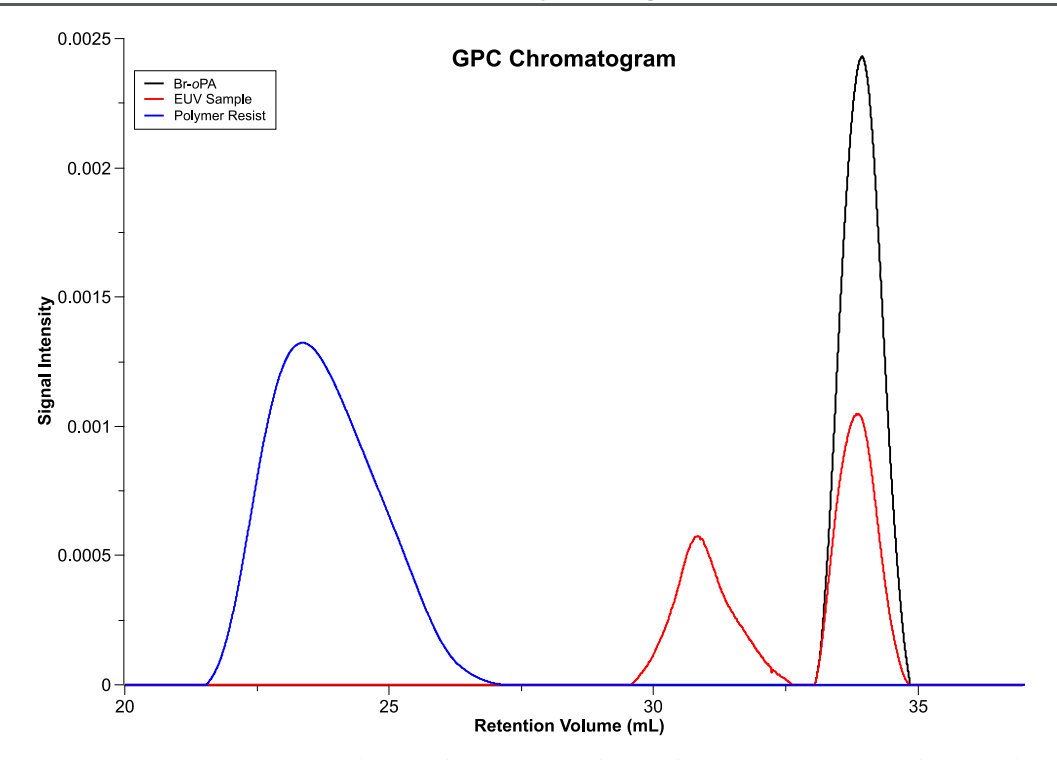


Figure 3. GPC chromatogram of the polymer resist (blue plot), EUV sample (red plot), and Br-oPA monomer (black plot).

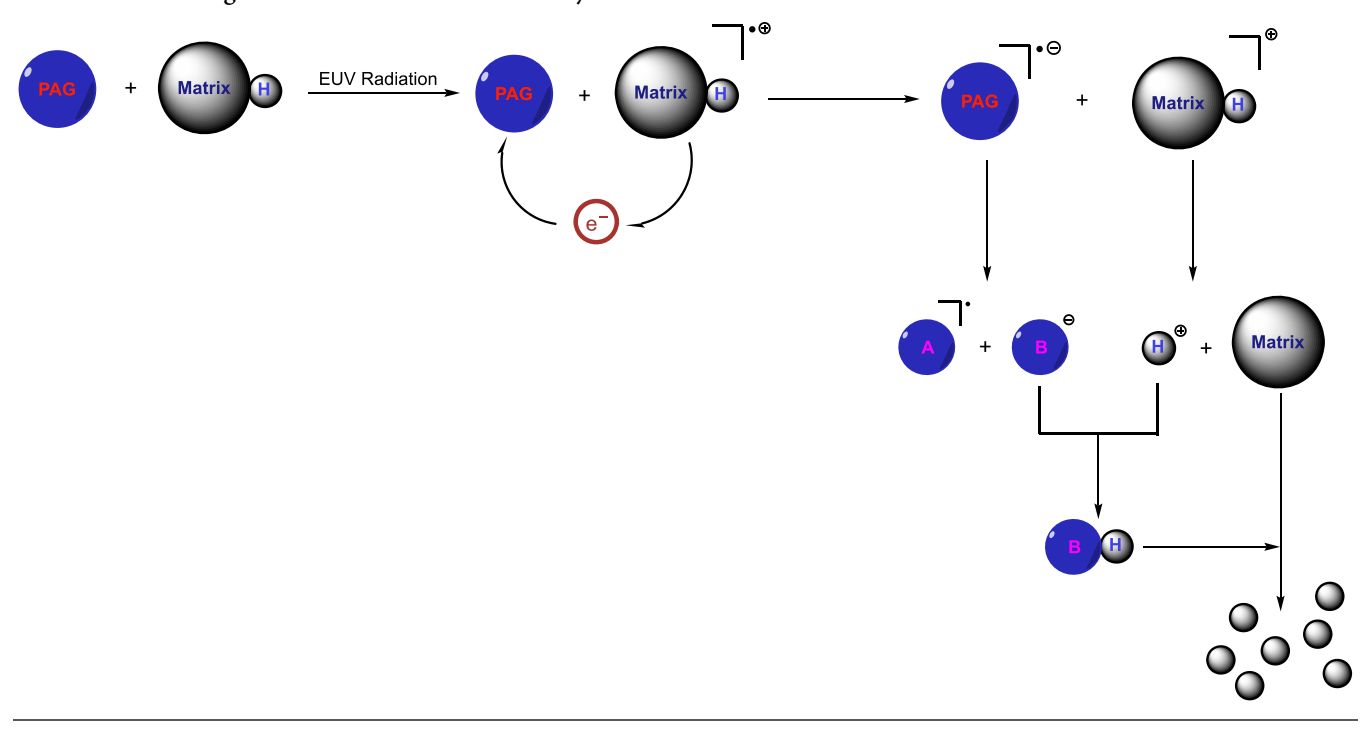
evaluated under DUV exposures using an ASML DUV stepper. The contrast curves are shown in Figure 1. These newly synthesized photoresist systems were evaluated for ideal soft and postexposure bake conditions as well as development solvent. Optimal soft and postexposure bake temperatures and times were found to be 90 °C for 1 min and 110 °C for 1 min, respectively. Of the development solvents evaluated, it was found that toluene, methanol, and isopropanol could preferentially dissolve the monomers, with isopropanol displaying the highest selectivity. It is important to note that all PAGs were soluble in isopropanol in the range of 52-86 mg/mL. Considering 250 mL was used for development, this allowed us to disregard the possibility of dissolution inhibition effects by the PAGs on the sensitivity of each resist system. To ensure that pattern formation occurred successfully, a line space pattern from PAG 3 was characterized by SEM and is shown in Figure S3. It is notable that the DUV sensitivity of the PAG 4 system was comparable to the original PPA<sup>25</sup> (which utilized ionic PAGs) despite the significant increase in the stability of the polymer and the use of a nonionic PAG.

**EUV Exposure.** With the optimal processing conditions from the DUV experiments in hand, PAGs 3-9 were evaluated under EUV exposure. The EUV contrast curves are shown in Figure 2 with a log-scale version given in the Supporting Information (Figure S9). As noted previously, Br-IPPA did not show any significant activity by itself. This was unexpected as brominated, aromatic polymers have been shown to generate HBr (p $K_3$  -9.0) under e-beam conditions.<sup>53</sup> We suspected that the assumption that radical anion formation in both e-beam and EUV involves only thermalized electrons was not correct, and the absence of Br was indicative of the lower average energy of secondary electrons in EUV. The acid generated by PAGs 3–8 was retained as 4-bromobenzenesulfonic acid (p $K_a$ -3.1) because it had been sufficient to depolymerize Br-lPPA under DUV exposure based on the results of PAG 4. It was also appealing as very few EUV resists have been able to avoid

using fluorinated acids, which are of significant environmental concern. 54-56 We systematically designed PAGs 3-8 to possess a wide range of electron affinities and bond strengths to evaluate the relationship between chemical structure and EUV sensitivity. As we sought to elucidate the sensitivity trend of PAGs 3-8, the dependence of Br-IPPA's dose-to-clear on the concentration of PAGs generating 4-bromobenzenesulfonic acid was evaluated. The results are shown in Figure S10. Considering the spread in sensitivity of Br-lPPA was only 2 mJ/cm<sup>2</sup> across a PAG concentration range of 10 wt % (97 mol %), and the average difference in concentration of PAGs 3–8 in the resist systems was 21 mol % with a maximum difference of 72 mol %, the variations in PAG concentration could be safely discounted when exploring the origin of sensitivity differences between PAGs 3-8. PAG 5 merits special attention as it was recently shown to function as an initiator for photopolymerization of epoxides at the EUV wavelength<sup>57</sup> and has been highlighted by others<sup>52,58</sup> as a promising candidate for EUV lithography. As the generated photoacid of PAG 5 is approximately 10<sup>2</sup> times stronger than the acid (p-toluenesulfonic acid,  $pK_a - 1.3$ ) generated by the referenced PAG, <sup>57</sup> we expected PAG 5 to display even better performance under EUV exposure. From the contrast curve, all PAGs except for the aryl sulfonates, PAG 3 and 5, achieved dose-to-clear exposures below 25 mJ/cm<sup>2</sup>. PAG 5 did not possess sufficient sensitivity to merit its use in EUV photoresists. It is also noteworthy that the DUV active PAG 3 displays no similar activity under EUV. Both naphthalimide sulfonate PAGs, PAG 4 and 9, displayed highly unusual behavior in which a plateau was observed in their contrast curves, prompting the further mechanistic investigation.

The p $K_a$  of the acid generated by PAG 9 was dramatically lowered relative to PAGs 3–8 by nearly twelve units to assess if the resists still maintained a strong dependency on acid strength. While the increased EUV sensitivity of PAG 9 demonstrated this dependence was still present, it was

Scheme 5. PAG Degradation Mechanism Induced by EUV Photons



Scheme 6. Proposed Decomposition Mechanism of PAG 9 under EUV Radiation

significantly diminished compared to most deprotection-based CAR resists  $^{59}$  as the sensitivity only doubled compared to that of PAG 4 despite the  $10^{12}$  increase in acid strength. Additionally, the higher diffusion constant of triflic acid (p $K_{\rm a}$  -14.9) may have contributed to the increased sensitivity relative to the bulkier 4-bromobenzenesulfonic acid. Lastly, simple bromination of the imino phenyl ring on PAG 8 resulted in it nearly doubling its sensitivity compared to PAG 7. The results indicated that small structural changes could drastically alter EUV performance.

Mechanistic Study. To gain insight into the plateau observed in the contrast curve for PAG 4 and 9, the degradation pathway of the naphthalimide PAG was studied. A wafer coated with Br-lPPA resist and PAG 9 was exposed to EUV radiation at the dosage of 3 mJ/cm² and postbaked at 110 °C for 1 min. The wafer was then developed in isopropanol for 1 min. The development solution was concentrated *in vacuo* and used for gel permeation chromatography (GPC) and mass spectrometry (MS) analysis. The GPC chromatogram is shown in Figure 3. The GPC chromatograms of the brominated *σ*PA monomer and the polymer resist are also shown for comparison. In Figure 3, two peaks were detected for the sample exposed under EUV (shown in the red curve). The first and second peaks had

relative molecular weights of 387 and 252 amu, respectively. The same sample was analyzed by mass spectrometry (Supporting Information, Figures S4–S6).

From the mass spectrum (Supporting Information, Figures S4–S6), three compounds were observed. The first peak appeared at m/z = 170.05996, which corresponded to the compound benzo[cd]indol-2(1H)-one. The second peak was at m/z = 212.95367, and the isotopomer pattern indicated the presence of a Br atom in the molecule, corresponding to the monomer Br-oPA. The third peak emerged at m/z = 345.99878, which corresponded to PAG 9. PAGs are known to decompose under EUV exposure by absorbing lower energy secondary electrons as shown in Scheme 5.  $^{10}$ 

The resist matrix plays the role of electron donor by absorbing EUV photons and ejecting a photoelectron. These primary photoelectrons possess enough energy to eject additional secondary electrons from the resist that diffuse away from the initial excitation point until they reach thermalization. The PAG accepts ejected electrons from the resist matrix, resulting in the formation of a radical anion. The radical anion decomposes to form radical A and anionic species B, which deprotonates the resist matrix to release the corresponding photoacid. The generated photoacid will in turn cause the resist matrix to depolymerize.

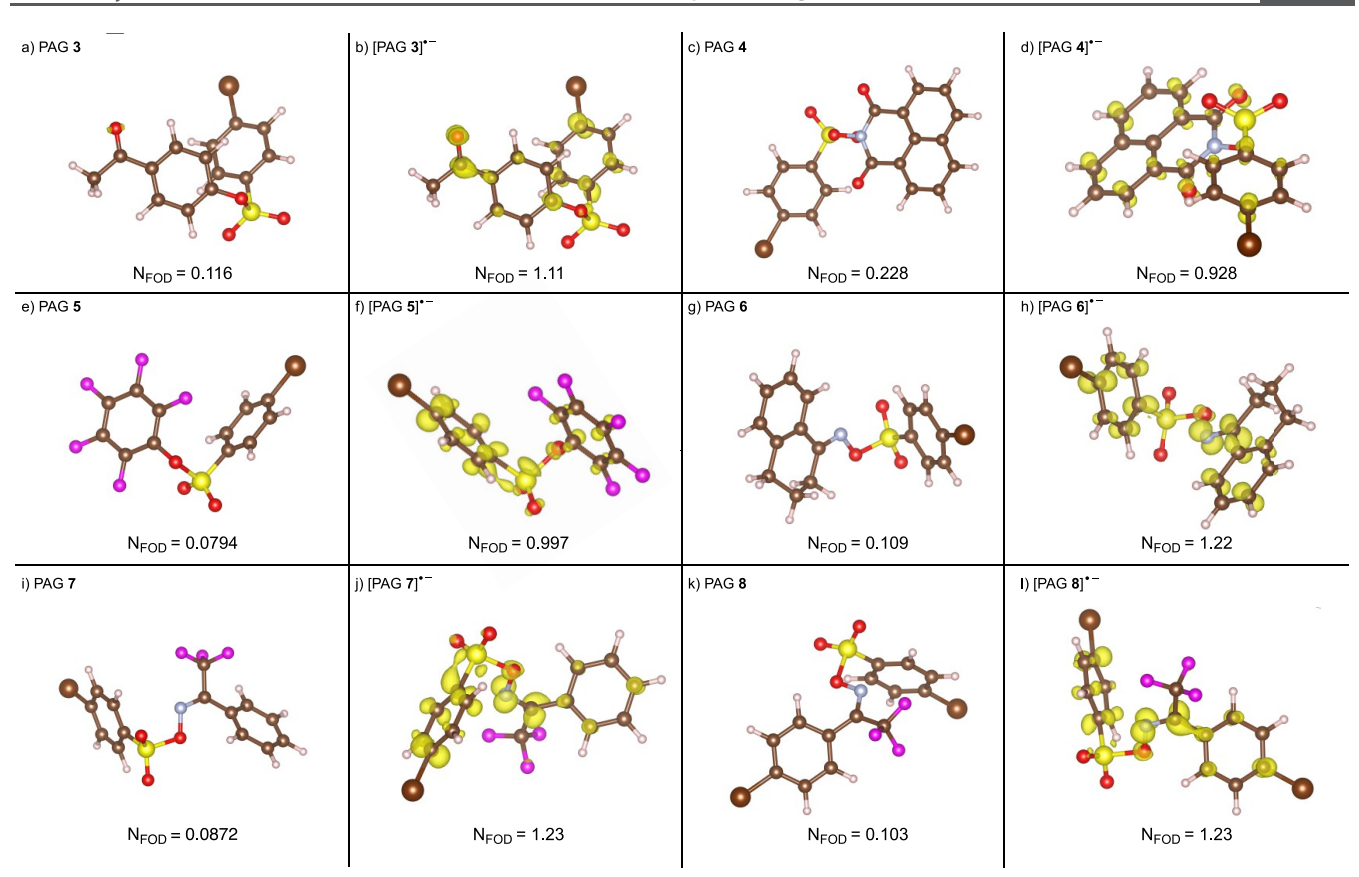


**Figure 4.** FOD plots at  $\sigma = 0.005$  e Bohr<sup>-3</sup> (FT-B97M-V/def2-TZVPP ( $T_{\rm el} = 5000$  K) level) for neutral and radical anions of PAG 3 to 8 (FOD in yellow).

Table 1. Table Summarizing Results of EA, Photospeed, Bond Dissociation Energy, and  $\Delta G^{\ddagger}$  for PAG 3 to 8.

PAG	vertical electron affinity (kcal/mol)	photospeed (mJ/cm <sup>2</sup> )	N-O BDE <sup>a</sup> (kcal/mol)	S-O BDE (kcal/mol)	$\Delta G^{\ddagger}$ (kcal/mol)
PAG 3	39.8	N/A	64.5	29.7	N/A
PAG 4	49.9	15	14.1	29.4	9.15
PAG 5	37.5	N/A	58.5	26.5	N/A
PAG 6	32.7	14	17.8	26.6	16.6
PAG 7	38.6	23	14.9	22.3	43.0
PAG 8	43.1	12	14.4	21.6	25.2
<sup>a</sup> For PAG 3 and 5 it is the C-O BDE					

Based on the compounds detected in the EUV exposed resist film and prior information on the EUV process, a rational decomposition mechanism was proposed for PAG 9 in Scheme 6. Remarkably, the PAG simultaneously generates both an acid and a lactam that acts as a quencher. This is significant as quencher distribution has been shown to be the most detrimental stochastic aspect of photoresist systems and could be avoided by having the same component generate both acid and base. The EUV mechanism also contrasts with its accepted mechanism under DUV irradiation in which homolytic bond cleavage occurs.

**DFT Calculations.** To understand the observed sensitivity trend under EUV exposure and shed light on the design of high sensitivity PAGs for EUV lithography, DFT calculations were conducted. According to the proposed reaction mechanism shown in Scheme 6, the acid generation efficiency is related to the reducibility of the PAGs. This trend has been verified experimentally <sup>34,40,41</sup> and computationally <sup>42</sup> in e-beam lithography. Additionally, PAG reduction potentials have been shown to correlate linearly with their vertical electron affinities

(VEAs). 46 Therefore, DFT calculations were first conducted to evaluate the VEAs of PAGs 3–8.

The calculation of the VEAs involves radical anion species, which is challenging as they show strong multireference character (alternatively termed strong static electron correlation (SEC)), which cannot be adequately described by standard single-reference DFT as SEC brings capricious effects into electronic wave functions and derived properties. First, to gauge the strongly correlated and chemically active electrons in the radical anions of the PAGs, fractional occupation number weighted density (FOD) analysis was performed. <sup>63</sup> The results are shown in Figure 4.

The single size-extensive number,  $N_{\rm FOD}$ , is the integration of the FOD over all space, which was established by Grimme et al. to globally quantify SEC.  $N_{\rm FOD}$  for all radical anions is far above the threshold value (0.2) between a single and multireference system indicating the strong multireference nature of these species. From the FOD plots, significant and delocalized FODs were seen in all radical anions, demonstrating that these species represent true multiconfigurational

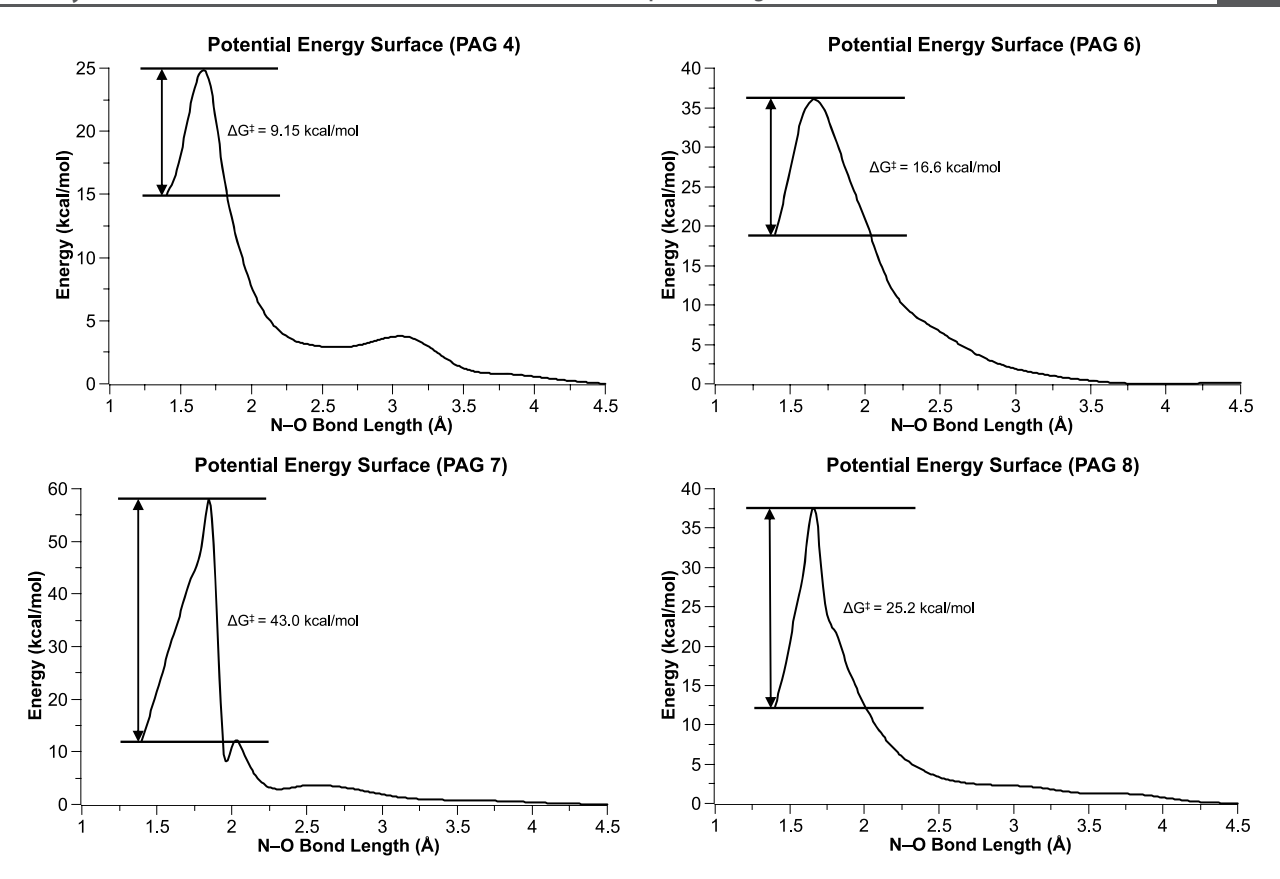


Figure 5. Potential energy surfaces along the N–O bond calculated at FT-TPSS-D4/def2-SVP ( $T_{\rm el}$  = 5000 K) level for PAG 4, 6, 7, and 8.

systems. It is noteworthy that in radical anions of PAGs 6, 7, and 8, a pronounced FOD was observed on the N–O bond, whereas for radical anions of PAG 3 and 5, the pronounced FOD was observed on the S–O bond. This could indicate that the most favorable bond cleavage site on PAGs 3 and 5 does not result in the production of a strong acid, which is supported by our contrast curve data. To obtain reliable molecular energies and structures for these multiconfigurational systems, Fermi-Smearing DFT (FT-DFT) with the meta GGA functional TPSS ( $T_{\rm el} = 5000~{\rm K}$ ), <sup>64</sup> combined with D4 dispersion correction, <sup>65</sup> the def2-SVP basis set and the gCP empirical counterpoise correction were utilized for geometry optimizations and thermal corrections. The final energies were calculated at the FT-B97M-V/def2-TZVPP ( $T_{\rm el} = 5000~{\rm K}$ ) level. <sup>66</sup> The calculated VEAs are summarized in Table 1.

As PAG 3 and PAG 5 were not active under the range of the applied doses, comparing their VEAs has no meaning. In order to compare the relative photospeeds of PAGs 4, 6, 7, and 8, the production of the internal base quencher in PAG 4 must be taken into account. We estimate the photospeed of PAG 4 based on its initial slope prior to the effect of quencher formation. PAGs 4 and 8 were found to possess the highest and second-highest VEAs, respectively, matching their photospeeds. The VEA relationship to photospeed appears to collapse when PAGs 6 and 7 are compared. While PAG 7 has the third-highest VEA among PAGs 4, 6, 7, and 8, its photospeed is significantly slower than all others. Although photospeed is highly correlated to VEA under e-beam, 40-43 such a relationship has not been as consistent under EUV.

To determine if other parameters correlated with the photospeed of the PAGs, we calculated the N-O bond dissociation energy (BDE), S-O BDE, and kinetic energy

barrier of the N-O bond dissociation of the radical anion for each PAG (Table 1). The BDE has previously been used to rationalize the favorability of dissociative electron transfer processes<sup>67</sup> as the kinetic barrier of such reactions is quadratically related to BDE via the well-known Marcus relationship.<sup>68</sup> Based on the N-O BDE, a favorable trend with photospeed was found for PAGs 4 and 8. However, the calculated N-O BDE still could not explain the trend for PAG 6 and 7. Despite this failure, it is clear that the N-O cleavage pathway is more favorable than the S-O cleavage for PAGs 4. 6, 7, and 8 and significantly more unfavorable (C–O cleavage) for PAGs 3 and 5. This agrees with the experimental data that shows that PAG 3 and 5 are not EUV active as S-O cleavage does not lead to the formation of a strong acid. The potential energy surfaces (PESs) along the N-O bond are shown in Figure 5 and demonstrate significant differences in the activation energy of the radical anion of the PAG dissociation process. While the VEAs of all PAGs suggest that near 0 eV, electrons readily attach<sup>69–71</sup> to the PAGs, the PESs reveal that such electrons would be insufficient to cause some of the PAGs to dissociate. For instance, while it is feasible that a thermalized electron could cause PAG 4 to undergo dissociation, this is not possible with PAG 7, which would require a secondary electron possessing ~1.86 eV to dissociate. In spite of this high barrier, PAG 7 is still very active under EUV exposure. This clashes with the widespread perception that PAGs react almost exclusively with thermalized electrons to dissociate, and that higher energy processes can be safely discounted. 10,46,72 Clearly, this assumption fails here. To obtain a single parameter that estimates the overall rate of the dissociative electron transfer process (Scheme 7), we combine the VEA

and kinetic barrier of the N-O bond cleavage to create an empirical relationship with photospeed shown in Figure 6.

## Scheme 7. Scheme Showing the Dissociative Electron Transfer Process

$$A-B+e^ A-B^ A^-+B^-$$

As can be seen, the correlation between this estimation of total activation energy and photospeed is excellent.

#### CONCLUSIONS

A series of photoresists based on acid-labile poly(acetal) polymers have been synthesized through anionic polymerizations of brominated oPA monomers. These Br-lPPA polymers were found to possess significantly improved thermostability in comparison to the original cPPA. The superior thermostability of Br-lPPA enabled higher postexposure bake temperatures to be applied and prevented previously catastrophic outgassing issues. As an initial starting point, the accompanying PAGs for each resist were designed based on functional groups that displayed high activity under DUV. Each PAG was synthesized using simple condensation reactions giving quantitative yields. DUV exposures were used to optimize processing conditions for the photoresist formulations. While both aryl and imino/imido sulfonate PAGs were found to be DUV active, only imino/imido sulfonate PAGs possessed high EUV sensitivity. Five derivatives displayed sensitivities well within commercial processing requirements. Two of the imidosulfonate PAGs displayed an unusual plateau region in their contrast curves that was further investigated through mechanistic studies employing GPC and MS analysis. Significantly, it was found that the naphthalimide sulfonate moiety could simultaneously

produce acid and base quencher under EUV exposure, a consequential discovery for the future development of photoresists. In DFT calculations, the focus was given to the most promising PAGs 4, 6, 7, and 8. VEA, BDE, and  $\Delta G^{\dagger}$  were calculated. By combining the VEA and  $\Delta G^{\dagger}$ , we obtained a single parameter that correctly predicts the overall rate of the dissociative electron transfer process and, by extension, the sensitivity of the resist. This parameter is currently being utilized in our research group in the development of single-component resists based on poly(acetal) polymers and the results will be reported in due course.

#### EXPERIMENTAL SECTION

Synthesis of Linear Brominated Polyphthalaldehyde (Br-IPPA). Linear brominated polyphthalaldehyde (Br-IPPA) was synthesized through anionic polymerization reactions. To a Schlenk flask charged with a magnetic stir bar evacuated and back-filled with N<sub>2</sub> three times was added the brominated phthalaldehyde monomer (10 mmol) and 4-biphenylmethanol (0.2 mmol) in the degassed anhydrous THF (20 mL) and cooled to -78 °C. 1,8-Diazabicyclo [5.4.0] undec-7-ene (DBU) (0.3 mmol) was added, and the reaction was left stirring at -78 °C for 4 h, then pyridine (3 mmol) and phenyl chloroformate (1.5 mmol) was added. The mixture was left stirring for 3 h at -78 °C, then warmed to room temperature, and the polymer was precipitated by adding the mixture slowly into methanol (100 mL). The white powders were collected by filtration, then further purified by dissolving in dichloromethane, reprecipitating from methanol, and washing in diethyl ether. The analytically pure product was obtained with 78% yield. <sup>1</sup>H NMR (500 MHz, DMSO):  $\delta$  8.15–7.05 (br, 3H, aromatic), 7.02–6.30 (br, 2H, acetal)

Synthesis of Aryl Sulfonate PAGs. To a round bottom flask charged with a magnetic stir bar and an addition funnel evacuated and back-filled with  $N_2$  three times was added the chosen phenol (20 mmol) in degassed anhydrous dichloromethane (80 mL) and triethylamine (15 mL) at room temperature. The chosen sulfonyl

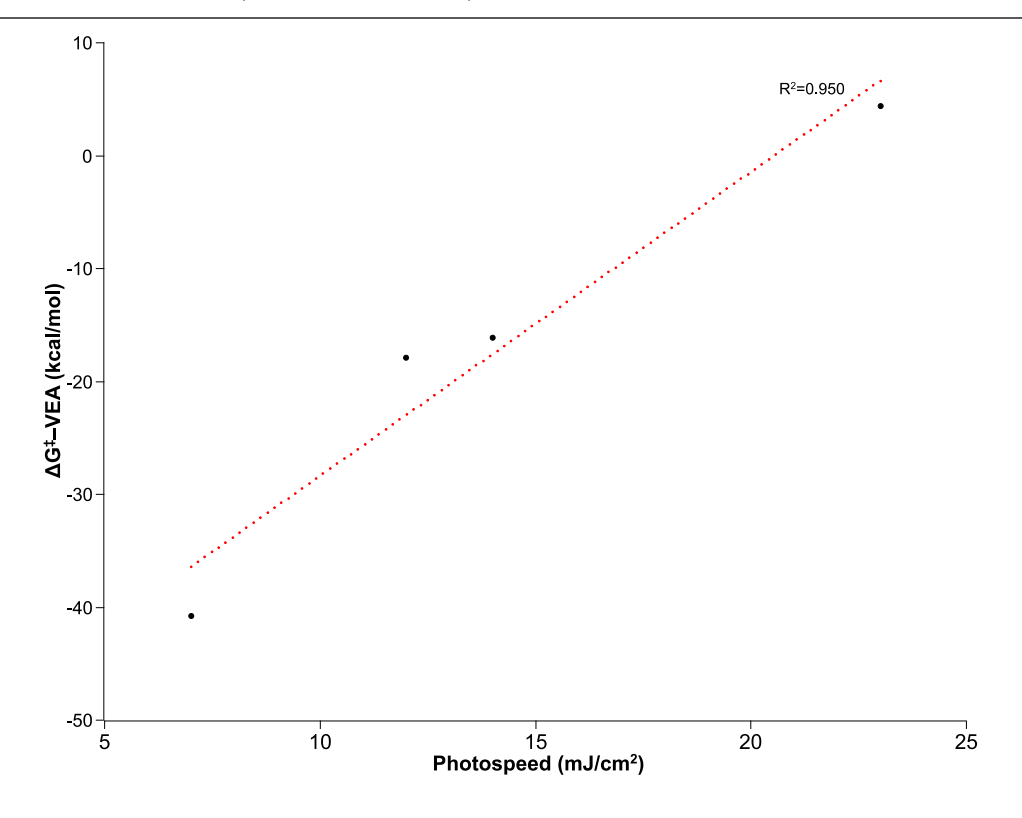


Figure 6. Empirical relationship between VEA corrected activation energy and photospeed.

chloride (24 mmol) was added dropwise via the addition funnel. The reaction was stirred at room temperature overnight. The reaction mixture was quenched by the addition of DI water (30 mL). The aqueous layer was separated and extracted with ethyl acetate (2  $\times$  50 mL). The organic layers were combined, washed with brine (100 mL), dried over MgSO<sub>4</sub>, and filtered and concentrated in vacuo. The crude product was purified by flash column chromatography rapidly to afford the corresponding aryl sulfonate.

Synthesis of Oxime/Naphthalimide Sulfonate PAGs. To a round bottom flask charged with a magnetic stir bar and an addition funnel evacuated and back-filled with N<sub>2</sub> three times was added the chosen oxime/N-hydroxy-1,8-naphthalimide (20 mmol) in degassed anhydrous dichloromethane (80 mL) and triethylamine (15 mL) at room temperature. The flask was then cooled to 0 °C via a water/ice bath. The chosen sulfonyl chloride (24 mmol) was added dropwise via the addition funnel. The reaction was stirred at room temperature overnight. The reaction mixture was quenched by the addition of DI water (40 mL). The aqueous layer was separated and extracted with ethyl acetate (2 × 50 mL). The organic layers were combined, washed with brine (100 mL), dried over MgSO<sub>4</sub>, and filtered and concentrated in vacuo. The crude product was purified by flash column chromatography rapidly to afford the corresponding imino/imido sulfonate.

**Photoresist Coating Conditions.** Photoresist polymers (35 mg) and PAGs (7 mg) were dissolved in 1 mL cyclohexanone. The resist was spin-coated onto a silicon wafer at 2500 rpm for 1 min resulting in film thickness of 50 nm and then soft baked on a hot plate at 90  $^{\circ}$ C for 1 min to remove residual casting solvent from the film.

**Deep-UV Exposure.** Deep-UV (DUV) exposures were conducted using ASML 300C DUV Wafer Stepper at the wavelength of 248 nm.

**Extreme-UV Exposure.** Extreme-UV (EUV) exposures at the wavelength of 13.5 nm were conducted using EUV tools at Intel Corporation.

#### ASSOCIATED CONTENT

#### Supporting Information

The Supporting Information is available free of charge at https://pubs.acs.org/doi/10.1021/acs.chemmater.2c01444.

The general procedures, synthetic and characterization details, TGA analysis, SEM characterization of patterns for DUV lithography, MS experiments, outgassing experiments, supplemental EUV contrast curves, PAG concentration table, NMR spectra, as well as computational details.(PDF)

#### AUTHOR INFORMATION

#### **Corresponding Authors**

Jingyuan Deng – Department of Chemistry and Chemical Biology and Department of Materials Science and Engineering, Cornell University, Ithaca, New York 14853, United States; orcid.org/0000-0002-0858-9919; Email: jd966@cornell.edu

Christopher K. Ober — Department of Materials Science and Engineering, Cornell University, Ithaca, New York 14853, United States; orcid.org/0000-0002-3805-3314; Email: cko3@cornell.edu

#### **Authors**

Sean Bailey – Department of Materials Science and Engineering and Department of Biomedical Engineering, Cornell University, Ithaca, New York 14853, United States; orcid.org/0000-0002-0792-210X

Shaoyi Jiang — Department of Materials Science and Engineering and Department of Biomedical Engineering, Cornell University, Ithaca, New York 14853, United States; orcid.org/0000-0001-9863-6899

Complete contact information is available at: https://pubs.acs.org/10.1021/acs.chemmater.2c01444

#### Notes

The authors declare no competing financial interest.

#### ACKNOWLEDGMENTS

This research was supported by Intel Corporation through the SRC research project (Task ID: 2885.001.) Exposures were performed at the Intel research facility. This work made use of the Cornell Center for Materials Research Shared Facilities which is supported through the NSF MRSEC program (DMR-1719875). In addition, characterization was performed at the Cornell NanoScale Facility, an NNCI member supported by NSF grant NNCI-2025233. The authors gratefully acknowledge the help from Intel collaborators, Dr. Grant Kloster, Dr. Patrick Theofanis, and Dr. Marie Krysak. In particular, we thank Dr. James Blackwell for the very helpful discussion and also for helping with various aspects of this work. We thank Prof. Gregory Denbeaux at SUNY POLY institute for the measurement of EUV outgassing experiments. S.J. and S.B. acknowledge start-up support from Cornell University, including Robert S. Langer Professorship and Cornell NEXT Nano Initiative.

#### REFERENCES

- (1) Yildirim, O.; Buitrago, E.; Hoefnagels, R.; Meeuwissen, M.; Wuister, S.; Rispens, G.; van Oosten, A.; Derks, P.; Finders, J.; Vockenhuber, M.; Ekinci, Y., *Improvements in Resist Performance towards EUV HVM*; SPIE, 2017; p 10143.
- (2) Li, L.; Liu, X.; Pal, S.; Wang, S.; Ober, C. K.; Giannelis, E. P. Extreme ultraviolet resist materials for sub-7 nm patterning. *Chem. Soc. Rev.* **2017**, *46*, 4855–4866.
- (3) Lee, S. M.; Frechet, J. M. J.; Willson, C. G. Photocrosslinking of Poly(4-hydroxystyrene) via Electrophilic Aromatic Substitution: Use of Polyfunctional Benzylic Alcohols in the Design of Chemically Amplified Resist Materials with Tunable Sensitivities. *Macromolecules* 1994, 27, 5154–5159.
- (4) Pasini, D.; Klopp, J. M.; Fréchet, J. M. J. Design, Synthesis, and Characterization of Carbon-Rich Cyclopolymers for 193 nm Microlithography. *Chem. Mater.* **2001**, *13*, 4136–4146.
- (5) Lin, Q.; Steinhäusler, T.; Simpson, L.; Wilder, M.; Medeiros, D. R.; Willson, C. G.; Havard, J.; Fréchet, J. M. J. A Water-Castable, Water-Developable Chemically Amplified Negative-Tone Resist. *Chem. Mater.* **1997**, *9*, 1725–1730.
- (6) MacDonald, S. A.; Willson, C. G.; Frechet, J. M. J. Chemical Amplification in High-Resolution Imaging Systems. *Acc. Chem. Res.* **1994**, *27*, 151–158.
- (7) Yu, T.; Ober, C. K.; Kuebler, S. M.; Zhou, W.; Marder, S. R.; Perry, J. W. Chemically Amplified Positive Resists for Two-Photon Three-Dimensional Microfabrication. *Adv. Mater.* **2003**, *15*, 517–521.
- (8) Ito, H.; Willson, C. G.; Frechet, J. H. J. New UV Resists with Negative or Positive Tone. 1982 Symposium on VLSI Technology. Digest of Technical Papers; IEEE, 1982; pp 86–87.
- (9) Itani, T.; Kozawa, T. Resist Materials and Processes for Extreme Ultraviolet Lithography. *Jpn. J. Appl. Phys.* **2013**, *52*, 010002.
- (10) Kozawa, T.; Tagawa, S. Radiation Chemistry in Chemically Amplified Resists. *Jpn. J. Appl. Phys.* **2010**, *49*, 030001.
- (11) Kozawa, T.; Oizumi, H.; Itani, T.; Tagawa, S. Assessment and Extendibility of Chemically Amplified Resists for Extreme Ultraviolet Lithography: Consideration of Nanolithography beyond 22 nm Half-Pitch. *Jpn. J. Appl. Phys.* **2011**, *50*, 076503.
- (12) Prabhu, V. M.; Kang, S.; VanderHart, D. L.; Satija, S. K.; Lin, E. K.; Wu, W.-l. Photoresist latent and developer images as probed by neutron reflectivity methods. *Adv. Mater.* **2011**, *23*, 388–408.

- (13) Wieberger, F.; Neuber, C.; Ober, C. K.; Schmidt, H.-W. Tailored star block copolymer architecture for high performance chemically amplified resists. *Adv. Mater.* **2012**, *24*, 5939–5944.
- (14) Chochos, C. L.; Ismailova, E.; Brochon, C.; Leclerc, N.; Tiron, R.; Sourd, C.; Bandelier, P.; Foucher, J.; Ridaoui, H.; Dirani, A.; Soppera, O.; Perret, D.; Brault, C.; Serra, C. A.; Hadziioannou, G. Hyperbranched Polymers for Photolithographic Applications Towards Understanding the Relationship between Chemical Structure of Polymer Resin and Lithographic Performances. *Adv. Mater.* **2009**, *21*, 1121–1125.
- (15) De Silva, A.; Felix, N. M.; Ober, C. K. Molecular Glass Resists as High-Resolution Patterning Materials. *Adv. Mater.* **2008**, *20*, 3355–3361.
- (16) Stocker, M. P.; Li, L.; Gattass, R. R.; Fourkas, J. T. Multiphoton photoresists giving nanoscale resolution that is inversely dependent on exposure time. *Nat. Chem.* **2011**, *3*, 223–227.
- (17) Li, L.; Gattass, R. R.; Gershgoren, E.; Hwang, H.; Fourkas, J. T. Achieving  $\lambda/20$  Resolution by One-Color Initiation and Deactivation of Polymerization. *Science* **2009**, 324, 910–913.
- (18) García-Fernández, L.; Herbivo, C.; Arranz, V. S. M.; Warther, D.; Donato, L.; Specht, A.; del Campo, A. Dual photosensitive polymers with wavelength-selective photoresponse. *Adv. Mater.* **2014**, 26, 5012–5017.
- (19) Kozawa, T.; Tagawa, S. Relationship between Normalized Image Log Slope and Chemical Gradient in Chemically Amplified Extreme Ultraviolet Resists. *Jpn. J. Appl. Phys.* **2010**, *49*, 06GF02.
- (20) Yu, A.; Liu, H.; Blinco, J. P.; Jack, K. S.; Leeson, M.; Younkin, T. R.; Whittaker, A. K.; Blakey, I. Patterning of tailored polycarbonate based non-chemically amplified resists using extreme ultraviolet lithography. *Macromol. Rapid Commun.* **2010**, *31*, 1449–1455.
- (21) Deng, J.; Ratanasak, M.; Sako, Y.; Tokuda, H.; Maeda, C.; Hasegawa, J.-y.; Nozaki, K.; Ema, T. Aluminum porphyrins with quaternary ammonium halides as catalysts for copolymerization of cyclohexene oxide and CO2: metal-ligand cooperative catalysis. *Chem. Sci.* **2020**, *11*, 5669–5675.
- (22) Ogata, Y.; Masson, G.; Hishiro, Y.; Blackwell, J. M. Scissionable polymer resists for extreme ultraviolet lithography. *Proc. SPIE* **2010**, 7636, 938–951.
- (23) Ober, M. S.; Romer, D. R.; Etienne, J.; Thomas, P. J.; Jain, V.; Cameron, J. F.; Thackeray, J. W. Backbone Degradable Poly(aryl acetal) Photoresist Polymers: Synthesis, Acid Sensitivity, and Extreme Ultraviolet Lithography Performance. *Macromolecules* **2019**, *52*, 886–895.
- (24) Deng, J.; Kaefer, F.; Bailey, S.; Otsubo, Y.; Meng, Z.; Segalman, R.; Ober, C. K. New Approaches to EUV Photoresists: Studies of Polyacetals and Polypeptoids to Expand the Photopolymer Toolbox. *J. Photopolym. Sci. Technol.* **2021**, *34*, 71–74.
- (25) Ito, H.; Willson, C. G. Chemical amplification in the design of dry developing resist materials. *Polym. Eng. Sci.* **1983**, 23, 1012–1018.
- (26) Rathore, A.; Pollentier, I.; Kumar, S. S.; De Simone, D.; De Gendt, S. Feasibility of unzipping polymer polyphthalaldehyde for extreme ultraviolet lithography. *J. Micro/Nanopatterning, Mater., Metrol.* **2021**, *20*, 034602.
- (27) Engler, A.; Tobin, C.; Lo, C. K.; Kohl, P. A. Influence of material and process parameters in the dry-development of positive-tone, polyaldehyde photoresist. *J. Mater. Res.* **2020**, *35*, 2917–2924.
- (28) Wang, F.; Diesendruck, C. E. Polyphthalaldehyde: Synthesis, Derivatives, and Applications. *Macromol. Rapid Commun.* **2017**, 39, 1700519.
- (29) Joo, W.; Wang, W.; Mesch, R.; Matsuzawa, K.; Liu, D.; Willson, C. G. Synthesis of Unzipping Polyester and a Study of its Photochemistry. *J. Am. Chem. Soc.* **2019**, *141*, 14736–14741.
- (30) Lawrie, K. J.; Blakey, I.; Blinco, J. P.; Cheng, H. H.; Gronheid, R.; Jack, K. S.; Pollentier, I.; Leeson, M. J.; Younkin, T. R.; Whittaker, A. K. Chain scission resists for extreme ultraviolet lithography based on high performance polysulfone-containing polymers. *J. Mater. Chem.* **2011**, 21, 5629.
- (31) Kruger, S.; Revuru, S.; Higgins, C.; Gibbons, S.; Freedman, D. A.; Yueh, W.; Younkin, T. R.; Brainard, R. L. Fluorinated acid

- amplifiers for EUV lithography. J. Am. Chem. Soc. 2009, 131, 9862-
- (32) Kruger, S. A.; Higgins, C.; Cardineau, B.; Younkin, T. R.; Brainard, R. L. Catalytic and Autocatalytic Mechanisms of Acid Amplifiers for Use in EUV Photoresists. *Chem. Mater.* **2010**, 22, 5609–5616.
- (33) Fedynyshyn, T. H.; Pottebaum, I.; Astolfi, D. K.; Cabral, A.; Roberts, J.; Meagley, R. Contribution of photoacid generator to material roughness. J. Vac. Sci. Technol., B: Microelectron. Nanometer Struct.—Process., Meas., Phenom. 2006, 24, 3031.
- (34) Lawson, R. A.; Noga, D. E.; Tolbert, L. M.; Henderson, C. L. Non-ionic PAG behavior under high energy exposure sources. *Proc. SPIE* **2009**, 7273, 524–532.
- (35) Martin, C. J.; Rapenne, G.; Nakashima, T.; Kawai, T. Recent progress in development of photoacid generators. *J. Photochem. Photobiol.*, C **2018**, 34, 41–51.
- (36) Higgins, C. D.; Szmanda, C. R.; Antohe, A.; Denbeaux, G.; Georger, J.; Brainard, R. L. Resolution, Line-Edge Roughness, Sensitivity Tradeoff, and Quantum Yield of High Photo Acid Generator Resists for Extreme Ultraviolet Lithography. *Jpn. J. Appl. Phys.* **2011**, *50*, 036504.
- (37) Lawson, R. A.; Lee, C.-T.; Yueh, W.; Tolbert, L.; Henderson, C. L. Single molecule chemically amplified resists based on ionic and non-ionic PAGs. *Proc. SPIE* **2008**, *6923*, 196–205.
- (38) Yueh, W.; Cao, H. B.; Thirumala, V.; Choi, H. Quantification of EUV resist outgassing. *Proc. SPIE* **2005**, *5753*, 765–770.
- (39) Gonsalves, K. E.; Thiyagarajan, M.; Dean, K. Newly developed polymer bound photoacid generator resist for sub-100-nm pattern by EUV lithography. *Proc. SPIE* **2005**, *5753*, 771–777.
- (40) Lee, C.-T.; Wang, M.; Gonsalves, K. E.; Yueh, W.; Roberts, J. M.; Younkin, T. R.; Henderson, C. L. Effect of PAG and matrix structure on PAG acid generation behavior under UV and high-energy radiation exposure. *Proc. SPIE* **2008**, *6923*, 755–762.
- (41) Yamashita, K.; Kamimura, S.; Takahashi, H.; Nishikawa, N. A Resist Material Study for LWR and Resolution Improvement in EUV Lithography. *J. Photopolym. Sci. Technol.* **2008**, 21, 439–442.
- (42) Okamoto, K.; Kozawa, T. Estimation of electron affinity of photoacid generators: density functional theory calculations using static and dynamic models. *Jpn. J. Appl. Phys.* **2021**, *60*, SCCC03.
- (43) Tarutani, S.; Tsubaki, H.; Tamaoki, H.; Takahashi, H.; Itou, T. Study on Approaches for Improvement of EUV-resist Sensitivity. *J. Photopolym. Sci. Technol.* **2010**, 23, 693–698.
- (44) Goldfarb, D. L.; Afzali-Ardakani, A.; Glodde, M. Acid generation efficiency: EUV photons versus photoelectrons. *Proc. SPIE* **2016**, 9779, 6–18.
- (45) Grzeskowiak, S.; Narasimhan, A.; Rebeyev, E.; Joshi, S.; Brainard, R. L.; Denbeaux, G. Acid Generation Efficiency of EUV PAGs via Low Energy Electron Exposure. *J. Photopolym. Sci. Technol.* **2016**, 29, 453–458.
- (46) Ma, J. H.; Wang, H.; Prendergast, D. G.; Neureuther, A. R.; Naulleau, P. P. Investigating extreme ultraviolet radiation chemistry with first-principles quantum chemistry calculations. *J. Micro/Nanolithogr., MEMS, MOEMS* **2020**, *19*, 034601.
- (47) Köstler, S.; Zechner, B.; Trathnigg, B.; Fasl, H.; Kern, W.; Ribitsch, V. Amphiphilic block copolymers containing thermally degradable poly(phthalaldehyde) blocks. *J. Polym. Sci., Part A: Polym. Chem.* **2009**, 47, 1499–1509.
- (48) Hernandez, H. L.; Kang, S.-K.; Lee, O. P.; Hwang, S.-W.; Kaitz, J. A.; Inci, B.; Park, C. W.; Chung, S.; Sottos, N. R.; Moore, J. S.; Rogers, J. A.; White, S. R. Triggered Transience of Metastable Poly(phthalaldehyde) for Transient Electronics. *Adv. Mater.* **2014**, *26*, 7637–7642.
- (49) Lutz, J. P.; Davydovich, O.; Hannigan, M. D.; Moore, J. S.; Zimmerman, P. M.; McNeil, A. J. Functionalized and Degradable Polyphthalaldehyde Derivatives. *J. Am. Chem. Soc.* **2019**, *141*, 14544–14548.
- (50) Schwartz, J. M.; Phillips, O.; Engler, A.; Sutlief, A.; Lee, J.; Kohl, P. A. Stable, High-Molecular-Weight Poly(phthalaldehyde). *J. Polym. Sci., Part A: Polym. Chem.* **2017**, *55*, 1166–1172.

- (51) Blakey, I.; Yu, A.; Blinco, J.; Jack, K. S.; Liu, H.; Leeson, M.; Yueh, W.; Younkin, T.; Whittaker, A. K. Polycarbonate based nonchemically amplified photoresists for extreme ultraviolet lithography. *Proc. SPIE* **2010**, *7636*, 952–959.
- (52) Manouras, T.; Argitis, P. High Sensitivity Resists for EUV Lithography: A Review of Material Design Strategies and Performance Results. *Nanomaterials* **2020**, *10*, 1593.
- (53) Yamamoto, H.; Kozawa, T.; Tagawa, S.; Ohmori, K.; Sato, M.; Komano, H. Single-Component Chemically Amplified Resist Based on Dehalogenation of Polymer. *Jpn. J. Appl. Phys.* **2007**, *46*, L648–L650
- (54) Ayothi, R.; Yi; Cao, H. B.; Yueh, W.; Putna, S.; Ober, C. K. Arylonium Photoacid Generators Containing Environmentally Compatible Aryloxyperfluoroalkanesulfonate Groups. *Chem. Mater.* **2007**, *19*, 1434–1444.
- (55) Ober, C.; Kafer, F.; Deng, J. Review of essential use of fluorochemicals in lithographic patterning and semiconductor processing. J. Micro/Nanopatterning, Mater., Metrol. 2022, 21, 010901.
- (56) Liu, S.; Glodde, M.; Varanasi, P. R. Design, synthesis, and characterization of fluorine-free PAGs for 193-nm lithography. *Proc. SPIE* **2010**, 7639, 112–119.
- (57) Torti, E.; Protti, S.; Bollanti, S.; Flora, F.; Torre, A.; Brusatin, G.; Gerardino, A.; Businaro, L.; Fagnoni, M.; Della Giustina, G.; Mezi, L. Aryl Sulfonates as Initiators for Extreme Ultraviolet Lithography: Applications in Epoxy-Based Hybrid Materials. *ChemPhotoChem* **2018**, *2*, 425–432.
- (58) Hao, C.; Wang, Q.; Wang, X.; He, X.; Xu, H. Towards Extreme Ultraviolet Lithography: Progress and Challenges of Photoresists. *Chin. J. Appl. Chem.* **2021**, *38*, 1154–1167.
- (59) Cameron, J. F.; Ablaza, S. L.; Xu, G.; Yueh, W. Design and Chemistry of Advanced Deep-UV Photoresists. The Role of the Photoacid Generator. J. Photopolym. Sci. Technol. 1999, 12, 607–620.
- (60) Kohmoto, S.; Motomura, T.; Takahashi, M.; Kishikawa, K. Stabilization of  $\gamma$ -lactam and lactone ring-fused norcaradienes by protonation: DFT calculations of norcaradiene and the corresponding cycloheptatriene structures. *J. Mol. Struct.* **2010**, 964, 47–51.
- (61) Naulleau, P.; Gallatin, G. Relative importance of various stochastic terms and EUV patterning. J. Micro/Nanolithogr., MEMS, MOEMS 2018, 17, 041015.
- (62) Malval, J.-P.; Suzuki, S.; Morlet-Savary, F.; Allonas, X.; Fouassier, J.-P.; Takahara, S.; Yamaoka, T. Photochemistry of Naphthalimide Photoacid Generators. *J. Phys. Chem. A* **2008**, *112*, 3879–3885.
- (63) Grimme, S.; Hansen, A. A Practicable Real-Space Measure and Visualization of Static Electron-Correlation Effects. *Angew. Chem., Int. Ed.* **2015**, *54*, 12308–12313.
- (64) Kanai, Y.; Wang, X.; Selloni, A.; Car, R. Testing the TPSS metageneralized-gradient-approximation exchange-correlation functional in calculations of transition states and reaction barriers. *J. Chem. Phys.* **2006**, *125*, 234104.
- (65) Caldeweyher, E.; Mewes, J.-M.; Ehlert, S.; Grimme, S. Extension and evaluation of the D4 London-dispersion model for periodic systems. *Phys. Chem. Chem. Phys.* **2020**, 22, 8499–8512.
- (66) Mardirossian, N.; Head-Gordon, M. Mapping the genome of meta-generalized gradient approximation density functionals: The search for B97M-V. *J. Chem. Phys.* **2015**, *142*, 074111.
- (67) Behar, D.; Neta, P. Intramolecular electron transfer and dehalogenation of anion radicals. 4. Haloacetophenones and related compounds. J. Am. Chem. Soc. 1981, 103, 2280–2283.
- (68) Antonello, S.; Maran, F. Intramolecular dissociative electron transfer. *Chem. Soc. Rev.* **2005**, *34*, 418–428.
- (69) Gu, J.; Wang, J.; Leszczynski, J. Electron attachment-induced DNA single strand breaks: C3'-O3' sigma-bond breaking of pyrimidine nucleotides predominates. J. Am. Chem. Soc. 2006, 128, 9322–9323.
- (70) Li, X.; Sanche, L.; Sevilla, M. D. Dehalogenation of 5-Halouracils after Low Energy Electron Attachment: A Density Functional Theory Investigation. *J. Phys. Chem. A* **2002**, *106*, 11248–11253.

- (71) Gu, J.; Xie, Y.; Schaefer, H. F., 3rd Near 0 eV electrons attach to nucleotides. *J. Am. Chem. Soc.* **2006**, *128*, 1250–1252.
- (72) Kozawa, T.; Yoshida, Y.; Uesaka, M.; Tagawa, S. Radiation-Induced Acid Generation Reactions in Chemically Amplified Resists for Electron Beam and X-Ray Lithography. *Jpn. J. Appl. Phys.* **1992**, *31*, 4301–4306.

### **□** Recommended by ACS

#### Extreme Ultraviolet-Printability and Mechanistic Studies of Engineered Hydrogen Silsesquioxane Photoresist Systems

Ashish Rathore, Stefan De Gendt, et al.

MARCH 04, 2021

ACS APPLIED POLYMER MATERIALS

READ 🗹

#### Bottom-Up Nanofabrication with Extreme-Ultraviolet Light: Metal-Organic Frameworks on Patterned Monolayers

O. Lugier, S. Castellanos, et al.

AUGUST 31, 2021

ACS APPLIED MATERIALS & INTERFACES

READ 🗹

# Biocompatible Silicon-Based Hybrid Nanolayers for Functionalization of Complex Surface Morphologies

Karina Ashurbekova, Mato Knez, et al.

FEBRUARY 15, 2022

ACS APPLIED NANO MATERIALS

READ 🗹

# Efficient and Controlled Seeded Growth of Poly(3-hexylthiophene) Block Copolymer Nanofibers through Suppression of Homogeneous Nucleation

Liam R. MacFarlane, Ian Manners, et al.

DECEMBER 06, 2021

MACROMOLECULES

READ 🗹

Get More Suggestions >